TSINGHUA SCIENCE AND TECHNOLOGY
ISSN 1007-0214 16/24 pp1509–1523
DOI: 10.26599/TST.2023.9010103
Volume 29, Number 5, October 2024

Acute Complication Prediction and Diagnosis Model CLSTM-BPR: A Fusion Method of Time Series Deep Learning and Bayesian Personalized Ranking

Xi Chen and Quan Cheng*

Abstract: Acute complication prediction model is of great importance for the overall reduction of premature death in chronic diseases. The CLSTM-BPR proposed in this paper aims to improve the accuracy, interpretability, and generalizability of the existing disease prediction models. Firstly, through its complex neural network structure, CLSTM-BPR considers both disease commonality and patient characteristics in the prediction process. Secondly, by splicing the time series prediction algorithm and classifier, the judgment basis is given along with the prediction results. Finally, this model introduces the pairwise algorithm Bayesian Personalized Ranking (BPR) into the medical field for the first time, and achieves a good result in the diagnosis of six acute complications. Experiments on the Medical Information Mart for Intensive Care IV (MIMIC-IV) dataset show that the average Mean Absolute Error (MAE) of biomarker value prediction of the CLSTM-BPR model is 0.26, and the average accuracy (ACC) of the CLSTM-BPR model for acute complication diagnosis is 92.5%. Comparison experiments and ablation experiments further demonstrate the reliability of CLSTM-BPR in the prediction of acute complication, which is an advancement of current disease prediction tools.

Key words: Long Short-Term Memory (LSTM); Bayesian Personalized Ranking (BPR); sudden illnesses; disease predictions

1 Introduction

41 million people die each year from Non-Communicable Diseases (NCDs), with over 40% of these deaths occurring prematurely[1]. Early mortality in NCDs is closely related to their acute complications, especially acute cerebral hemorrhage[2], acute heart failure[3], and acute renal failure[4]. Moreover, 77% of all NCD deaths are in low- and middle-income countries[5]. To achieve an overall reduction in premature death from NCDs, the application of artificial intelligence to predict acute complications is critical.

Artificial intelligence is inspired by biological processes, especially input processing approaches used by the human brain[6]. In a real-world medical scenario, the physician first has an overall understanding of a disease and then makes a diagnosis in conjunction with the specific patient condition, including the patient's current physical status, demographic information, and history of visits. Disease prediction models are expected to think the same way. The widespread establishment of Electronic Health Record (EHR) systems has provided data support for disease prediction models. Utilizing EHR, Zhang et al.[7] proposed the attention-based time-aware Long Short-Term Memory (LSTM) networks network. They focused on visits between 3 and 90 days among 1869 shock-positive and 231 shock-negative patients, using four categories of characteristics to predict whether infectious shock would occur. According to glucose readings, insulin bolus, and meal data, Li et al.[8]

• Xi Chen and Quan Cheng are with School of Economics and Management, Fuzhou University, Fuzhou 350108, China. E-mail: chenxiarya@163.com; chengquan@fzu.edu.cn.
* To whom correspondence should be addressed.
Manuscript received: 2022-12-16; revised: 2023-07-16; accepted: 2023-08-29

constructed a convolutional recurrent neural network to predict blood glucose changes in diabetic patients. Koo et al.[9] collected data on 7267 patients diagnosed with prostate cancer. Multi-layer perceptron for *N*-year survival prediction and LSTM models are used to predict prostate cancer survival outcomes according to initial treatment strategy. These disease prediction models not only help with early intervention and timely treatment, but also enable noninvasive monitoring and greatly reduce medical costs and discomfort[10, 11]. However, in these analogy-based disease prediction models, individual visit history is rarely considered. This leads to that disease prediction models take into account the commonalities of a disease but ignore the characteristics of the disease in a specific patient.

Meanwhile, the lack of interpretability and generalizability has hampered clinical use of disease prediction models. Dutta et al.[12] proposed a stacked GRU-LSTM-BRNN model, trained on a breast cancer dataset containing 357 benign and 212 malignant cases, to predict breast cancer impact using ten attribute values. Mohan et al.[13] produced a prediction model integrating a hybrid random forest with a linear model and achieved an enhanced performance accuracy (ACC) of 88.7% for heart disease diagnosis. First, these models only tend to predict whether a disease will occur or not. In fact, the next stage of biomarkers should receive more attention, which can provide a basis for diagnosis and more decision help to physicians. Second, like GRU-LSTM-BRNN for breast cancer, most models are designed for specific diseases, narrowing the application scope of the predictive models. Particularly in the field of acute complication prediction, on the one hand, prediction models for acute complications of chronic diseases are not well studied. On the other hand, acute complications of chronic diseases have some commonality and require a predictive model that can be generalized.

In this paper, we propose CLSTM-BPR, a predictive model for acute complications of multiple chronic diseases. To enhance model accuracy, a special CLSTM structure is designed to predict biomarker values using a combination of inter-patient cross-sectional EHR data and individual patient longitudinal EHR data. Then the ranking algorithm Bayesian Personalized Ranking (BPR) is introduced for the first time to diagnose the occurrence of acute complications based on predicted biomarker values and patient demographic information. As a validation of this model, the Medical Information Mart for Intensive Care IV (MIMIC-IV) medical dataset is chosen for the experiment. Six acute complications, including acute cerebral hemorrhage, acute heart failure, and acute renal failure are selected as separate predictive targets. The lowest Mean Absolute Error (MAE) of the numerical prediction of signs is 0.13 and the highest diagnostic prediction ACC is 97.7%. The experimental results demonstrate that the model can well predict whether acute complications will occur in patients with different chronic diseases and give the corresponding biomarker values.

2 Related Work

At present, the introduction of deep learning algorithms for disease prediction has become the main direction of research in this field. Compared to machine learning, deep learning based models tend to achieve better results in disease prediction[14, 15]. In particular, with powerful time-series feature processing capabilities, LSTM-based disease prediction models have been used for early disease detection[16], disease progression prediction[17], and survival prediction[18]. Among them, the deep learning architecture of hybrid Convolution Neural Network (CNN) and LSTM (CNN-LSTM) combines the advantages of CNN and LSTM to present better prediction results. Mahmudimanesh et al.[19] presented a new analysis and prediction model for the mortality of cardiovascular patients by considering air pollution indicators, demonstrating that CNN-LSTM provides more accurate results than classical methods, such as autoregressive integrated moving average model with exogenous regressors.

Although CNN-LSTM exhibits strong predictive power, it is not the best choice for diagnostic algorithms. Swapna et al.[20] presented a model for early detection of diabetes using CNN-LSTM to extract complex temporal dynamic features of the input data followed by Support Vector Machine (SVM) for classification. Compared to their earlier work that did not use SVM, the model achieves performance improvements of 0.06%, confirming that the combining CNN-LSTM with a classifier is effective. Prediction is a detection of the future. How to choose a more appropriate classifier for post-prediction diagnosis deserves further investigation.

Techniques like random forest[21, 22], K-nearest neighbors[22, 23], K-means[24], fuzzy logic[25], SVM[21−23, 26, 27], Decision Trees (DT)[23, 27], Logistic

Regression (LR)[26, 28], and Naive Bayes (NB)[22], help people diagnose many diseases. Classified from the perspective of processing data, the machine learning algorithms in these articles are all point-pair methods that transform diagnostic problems into classification and regression issues. By using the ranking algorithm BPR, CLSTM-BPR attempts to solve the disease diagnosis problem using a pairwise approach. To be specific, this model treats patient demographic information and predicted biomarkers as implicit feedback, and recommends a diagnosis by ranking the likelihood of an acute complication between two patients. The ability of BPR to handle implicit feedback from users has been widely demonstrated on implicit recommender systems[29, 30].

3 Methodology

3.1 Overview of the proposed method

The CLSTM-BPR acute complication prediction model proposed in this paper can be divided into two phases and five steps. In the prediction phase, by Model 1, the reciprocal n visit records of different patients are extracted in the public EHR to predict the patient biomarker value p_1 at the next visit. Secondly, the patient biomarker value p_2 at the next visit is obtained from Model 2 by using each of the m visit records in the individual EHR to predict the patient biomarkers value at $(m+1)$-th visits. Finally, p_1 and p_2 are concatenated to Model 3 to obtain the final biomarker information prediction result p_3. In the diagnosis phase, a BPR model is first trained by extracting the demographic information and biomarker information of patients with chronic diseases and patients who are suffering from acute complications. Then the demographic information and predicted biomarkers p_3 with the patient are fed into the trained BPR model to obtain the predicted diagnosis results. The overall research route is shown in Fig. 1.

3.2 CNN model

In reality, the doctor will first have a general understanding of the disease itself, and then guide the diagnosis based on previous experience in practicing medicine and the patient's past medical history. The CNN model serves this purpose. It is able to extract hidden features in physical sign data and medication data at each stage and combine them layer by layer to generate abstract high-level features. So that the subsequent LSTM model can process the features at each stage.

3.3 LSTM model

In this paper, we use LSTM to process the features extracted from CNN at each stage, which consists of a forget gate, input gate, and output gate[31]. First, the forget gate calculates the degree of forgetting of the previous cell. Then the input gate determines how

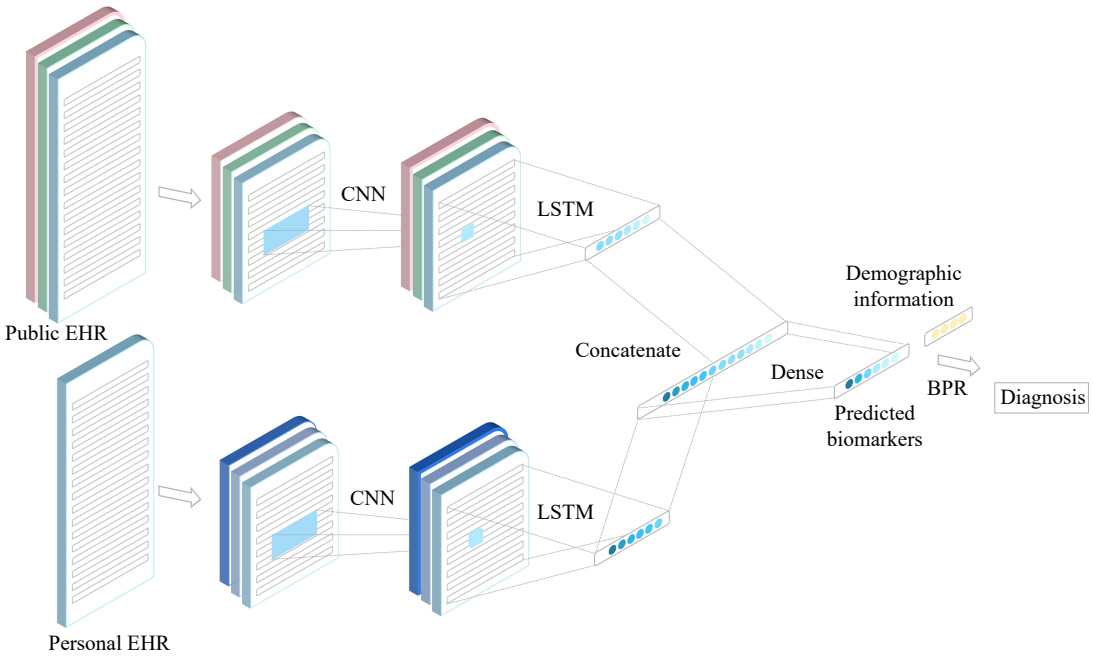

Fig. 1 Overall research roadmap.

much of these stage features need to be input into the cell to update the cell state. Finally, the output gate determines the part that needs to be output[32]. The structure of the LSTM network is shown in Fig. 2. The specific calculation formulas are as follows:

$$f_t = \sigma\left(W_f\left[h_{t-1}\ x_t\right] + b_f\right) \tag{1}$$

$$i_t = \sigma\left(W_i\left[h_{t-1}\ x_t\right] + b_i\right) \tag{2}$$

$$\tilde{C}_t = \tanh\left(W_c\left[h_{t-1}\ x_t\right] + b_c\right) \tag{3}$$

$$C_t = f_t \otimes C_{t-1} + i_t \otimes \tilde{C}_t \tag{4}$$

$$o_t = \sigma\left(W_o\left[h_{t-1}\ x_t\right] + b_o\right) \tag{5}$$

$$h_t = o_t \otimes \tanh\left(C_t\right) \tag{6}$$

where W_f, W_i, W_c, and W_o are the weight matrices; b_f, b_i, b_c, and b_o are the corresponding bias vectors; σ is the sigmoid function; tanh is the hyperbolic tangent function; $\otimes$ is the dot product; f_t is the retention degree value; i_t is the input degree value; o_t is the output degree value; x_t is the input of the current stage, that is, the features of each stage after CNN extraction; h_{t-1} is the output of the previous stage; h_t is the output of the current stage; C_{t-1} is the memory state of the previous stage; $\tilde{C}_t$ is the intermediate state; and C_t is the current state.

3.4 BPR

The disease diagnosis component determines whether a patient has a sudden onset of complication in the next stage through the predicted physical signs and demographic information of the patient. In this paper, this judgment is translated into comparing the weighted scores of abnormal signs and information items. First, disease set D is defined to consist of a certain emergent disease and its preexisting chronic disease. Patient set I, on the other hand, consists of patients with that emergent disease and patients with the preexisting disease. For the prediction ranking matrix corresponding to disease set D and patient set I, we expect to derive the disease to sign weighting matrix $W(|D|\times c)$, which satisfies the following equation with patient sign and information matrix S $(|I|\times c)$:

$$\hat{X} = W \times S^{\mathrm{T}} \tag{7}$$

where $\hat{X}$ is the set of likehood scores of patient i suffering from different diseases.

This model uses BPR to derive the weight matrix of diseases on signs. BPR is an algorithm that optimizes directly on ranking, and its goal is to rank the likelihood of patient confirmation for each disease. To do this, we introduce a triple $\langle d, i, j\rangle$, indicating that for disease d, patient i is more likely to be diagnosed than patient j. For disease d, the likelihood of patient i being diagnosed is denoted as

$$\hat{x}_{d,i}(\Theta) = w_d s_i = \sum_{f=1}^{k} w_{d,f} s_{i,f} \tag{8}$$

where w_d denotes the sign weight of disease d, s_i denotes the patient sign value and demographic information (e.g., age and gender), and Θ denotes all hyperparameters in the model, that is w_d in Eq. (8). The difference in the likelihood of patient i and patient j having disease d can be expressed as

$$\hat{x}_{d,i,j}(\Theta) = \hat{x}_{d,i}(\Theta) - \hat{x}_{d,j}(\Theta) \tag{9}$$

Let "$>d$" denote the full-order relationship of all patients corresponding to disease d, that is, all triples with respect to d. The initial optimization objective of the BPR model by the Bayesian probability formulation can be expressed as

$$\arg\max P(\Theta \mid > d) = \arg\max \frac{P(> d \mid \Theta) \times P(\Theta)}{P(> d)} \tag{10}$$

It is assumed that the ranking relationship of a disease is independent of other diseases, so that $P(>d)$ is a constant for disease d. It is also assumed that the prior distribution of the parameter Θ is a normal distribution $P(\Theta) \sim N(0, \lambda_\Theta I)$, where $\lambda_\Theta I$ denotes the variance. $P(>d|\Theta)$ can be rewritten as

$$\prod_{d\in D} P\left(> d \mid \Theta\right) = \prod_{(d,i,j)\in S} P\left(i > d_j \mid \Theta\right) \tag{11}$$

where S consists of all triads of disease d, that is, the all-order relationship for disease d. $P(i > d_j|\Theta)$ indicates that patient i is more likely to be diagnosed

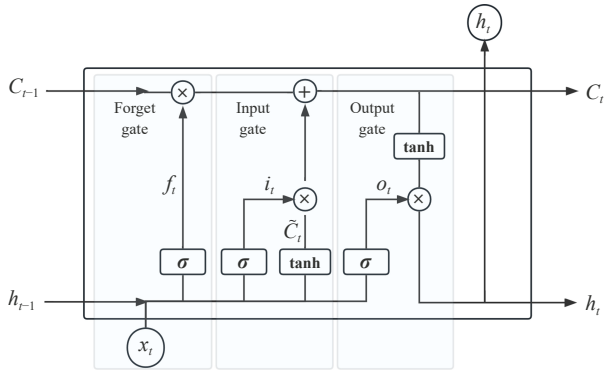

Fig. 2 LSTM structure diagram.

with disease d than patient j, conditional on parameter Θ. From Eq. (9), this greater likelihood can be expressed as

$$\prod_{d\in D} P\ (>d\,|\,\Theta) = \prod_{(d,i,j)\in S} \sigma\left(\hat{x}_{d,i}(\Theta) - \hat{x}_{d,j}(\Theta)\right) \tag{12}$$

Thus far, the objective function Eq. (10) can be transformed into

$$\arg\max \prod_{(d,i,j)\in S} \sigma\left(\hat{x}_{d,i}(\Theta) - \hat{x}_{d,j}(\Theta)\right) \times N(0,\lambda_\Theta I) \tag{13}$$

where $\sigma(x)$ is the sigmoid function.

Equation (13) can be transformed into the following equivalent optimization objective by means of a maximum log posterior estimation function:

$$\ln(P(\Theta|>d)) = \ln\left(\prod_{(d,i,j)\in S} \sigma\left(\hat{x}_{d,i}(\Theta) - \hat{x}_{d,j}(\Theta)\right)\right) + \lambda\,\|\Theta\|^2 \tag{14}$$

where $\lambda\,\|\Theta\|^2$ is the regularization term, λ denotes the regularization term coefficient, and $\|\cdot\|^2$ denotes the 2-norm. The parameters can be solved by the gradient descent method after taking the optimization objective function as negative. The iterative formula for the parameter Θ is as follows:

$$\frac{\partial\left(\ln\left(\prod_{(d,i,j)\in D} \sigma\left(\hat{x}_{d,i}(\Theta) - \hat{x}_{d,j}(\Theta)\right)\right) + \lambda\,\|\Theta\|^2\right)}{\partial(\Theta)} \propto \sum_{(d,i,j)\in D} \frac{1}{1+e^{\hat{x}_{d,i}(\Theta)-\hat{x}_{d,j}(\Theta)}} \times \frac{\partial\left(\hat{x}_{d,i}(\Theta) - \hat{x}_{d,j}(\Theta)\right)}{\partial(\Theta)} + \lambda\Theta \tag{15}$$

Due to

$$\hat{x}_{d,i}(\Theta) - \hat{x}_{d,j}(\Theta) = w_d\,(s_i - s_j) \tag{16}$$

Equation (15) can be derived that

$$w_d \leftarrow w_d + \alpha\left(\sum_{(d,i,j)\in D} \frac{1}{1+w_d\,(s_i-s_j)} \times (s_i - s_j) + \lambda\Theta\right) \tag{17}$$

where α denotes the learning rate.

Inputting the predicted sign values (p_3) and demographic information into the trained BPR model, the score of diagnosed diseases for patient i can be obtained,

$$x_{d,i}(\Theta) = w_d s_i = \sum_{f=1}^{k} w_{d,f}\, s_{i,f} \tag{18}$$

If the score of confirmed emergent diseases in patient i is greater than all preexisting diseases in disease set D, then it is determined that the patient will have an emergent disease in the next stage.

3.5 Sign prediction support technology

Figure 3 depicts the CLSTM-BPR neural network proposed in this paper, where formulas, such as "1 × 24" indicate the output size of each layer. The prediction part of the network consists of convolutional layer, pooling layer, LSTM layer, concatenated layer, and fully connected layer. The disease development features and individual features are extracted from the public EHR and individual EHR data by CNN-LSTM, respectively. After merging the common and individual features in the concatenate layer, the results are fed into the fully connected layer to predict the biomarker values at the next visit. In the diagnostic part, the BPR takes up the biomarker prediction values to judge whether acute complications will occur at the next visit for patients with chronic diseases.

The number of public EHR input visits, the number of individual EHR input visits, and the number of biomarker features differ for different acute complications. Figure 3 shows an example of acute cerebral hemorrhage with input size for Model 1 is 30 × 39 and Model 2 is 15 × 39. The CNN part consists of two CNN layers containing 32 and 64 filters with filter length 3 and activation function ReLU. Each CNN layer follows MaxPooling with a pool length of 2. Then the outputs of the CNN network are planarized as post-passed to the LSTM part, consisting of three LSTM layers with 64, 64, and 32 hidden units, respectively. The outputs of the LSTM network are concatenated into a 1 × 48 sequence after passing through a fully connected layer. Finally, 24 biomarker values are predicted after five fully connected layers with the number of neurons 256, 128, 64, 32, and 24. The activation function of the first four fully connected layers is ReLU, while the activation function of the last connected layer is linear.

4 Dataset

4.1 Dataset introduction

To verify the validity of this model, the MIMIC-IV medical dataset was chosen for the experiment. This dataset contains comprehensive information on patients hospitalized at an advanced academic medical center in

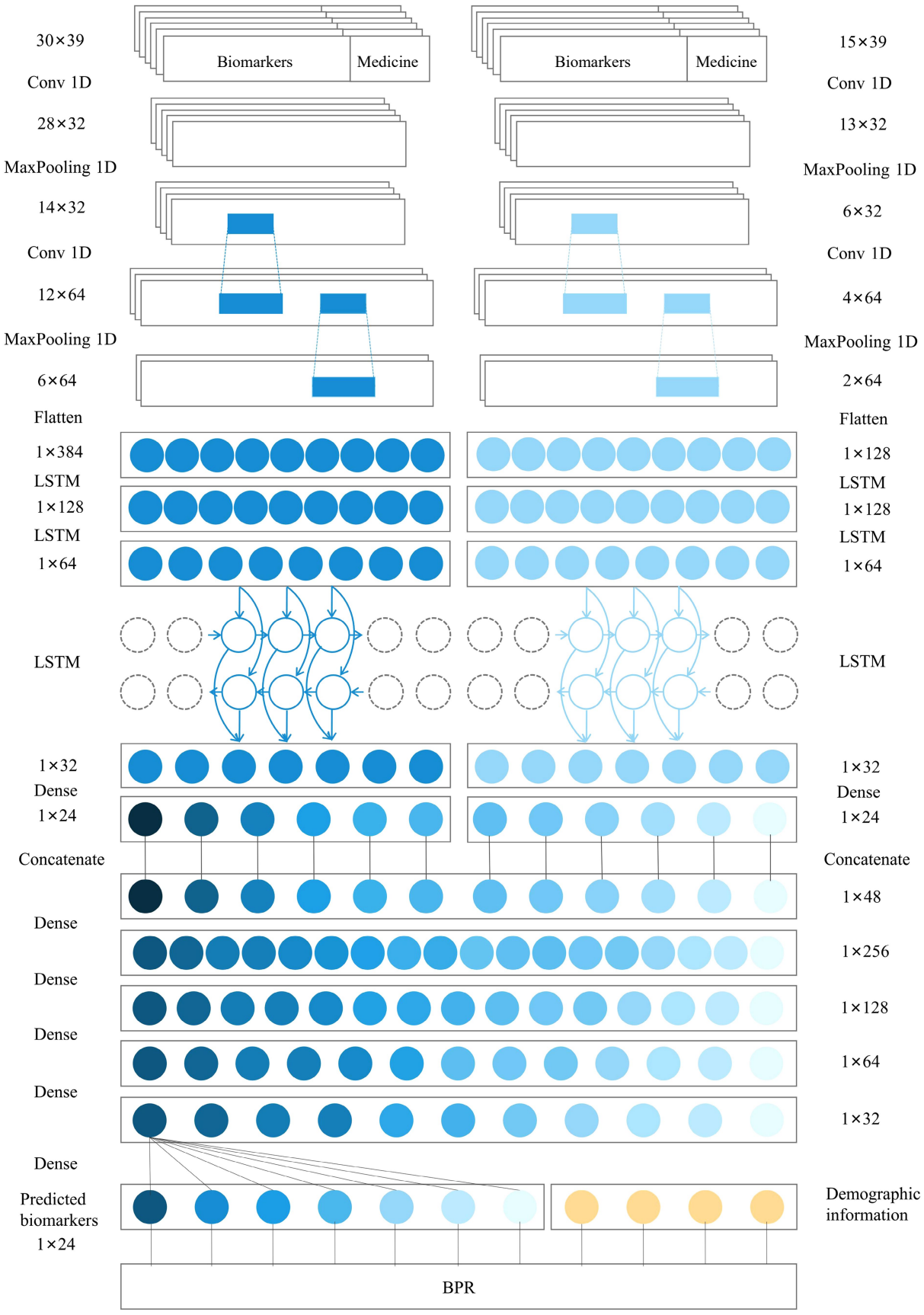

Fig. 3 Architecture of CLSTM-BPR.

Boston, Massachusetts, USA, such as laboratory measurements, medication records and admission information.

Cardiovascular diseases account for most NCD deaths, with 17.9 million people annually, followed by cancers (9.3 million), chronic respiratory diseases (4.1 million), and diabetes (2.0 million including kidney disease deaths caused by diabetes). These four groups of diseases account for over 80% of all premature NCD deaths[5]. Use these data as a reference, six acute complications with the highest number of patients are selected in MIMIC-IV: acute cerebral hemorrhage, acute heart failure, acute renal failure, acute pancreatitis, acute respiratory failure, and acute ketoacidosis. Then several preexisting chronic diseases with the highest number of people suffering from that acute complication are selected separately, as shown in Table 1.

For an acute complication, we need to extract those patients with chronic diseases that have been complicated by that acute complication, and those patients with chronic diseases that have not been complicated by that acute complication. The number of patients extracted under the condition of ensuring an adequate number of visits is shown in Table 2. In preparation for the BPR, age, height, weight, gender, marital status, and ethnicity of these patients are extracted.

When selecting biomarker characteristics, the 20 most examined biomarkers for all diagnoses of the acute complication and the 20 most examined biomarkers for all diagnoses of the preexisting chronic disease are selected. For drug characteristics, the 15 most frequently used drugs are selected for all diagnoses of the acute complication. The final biomarkers and drugs for each acute complication are shown in Tables 3 and 4. For patients without acute complications, all visit records are extracted since developing the preexisting chronic disease. For patients with acute complications, all visit records from the time of developing preexisting chronic disease to the first diagnosis of acute complications are extracted. Taking cerebral hemorrhage patient 14 731 854 as an example, the collated partial patient sign data are shown in Table 5, in which the physical signs data items are expressed with the codes in the d-labevent table of MIMIC-IV, such as 50868 for Anion Gap. Partial patient medication data are shown in Table 6, where "1" indicates medication, and "0" indicates no medication.

4.2 Dataset preprocessing

Because of differences in recording time, missing values occurred after combining the biomarker record sheet and the medication record sheet. Considering the actual treatment process, it often takes time for drugs to have their effect on patients. The missing values of biomarker records were filled by taking the most recent data in front. Considering that there is a limit on the number of times a drug can be used, the missing values

Table 1 Acute complications and preexisting chronic diseases comparison.

Acute complication	Preexisting chronic disease
Cerebral hemorrhage	Hypertension and hyperlipidemia
Heart failure	Chronic heart failure, atrial fibrillation, and coronary heart disease
Renal failure	Hypertensive chronic kidney disease, chronic kidney disease, and Type 2 diabetes
Pancreatitis	Hypertensive chronic kidney disease, chronic kidney disease, and Type 2 diabetes
Respiratory failure	Pneumonia, obstructive sleep apnea, obstructive chronic bronchitis, and hypothyroidism
Ketoacidosis	Type 1 diabetes with neurological complications, Type 1 diabetes with eye complications, and Type 1 diabetes mellitus with renal complications

Table 2 Acute complications and chronic disease abstraction numbers.

Acute complication	Patients with complication	Patients without complication	Total
Cerebral hemorrhage	58	70	128
Heart failure	92	100	192
Renal failure	28	50	78
Pancreatitis	73	100	173
Respiratory failure	113	137	250
Ketoacidosis	42	80	122

Table 3 Biomarker item.

Acute complication	Biomarker item
Cerebral hemorrhage	Glucose, pCO2, pH, pO2, Bicarbonate, Calcium (total), Chloride, Creatinine, Glucose (chemistry), Phosphate, Sodium, Urea Nitrogen, Hematocrit, Hemoglobin, INR(PT), MCH, MCHC, MCV, Platelet Count, PT, PTT, RDW, Red Blood Cells, White Blood Cells
Heart failure	Free Calcium, Glucose, Hemoglobin, pCO2, pH, pO2, Bicarbonate, Calcium (total), Chloride, Creatinine, Glucose, Phosphate, Troponin T, Urea Nitrogen, Hematocrit, Hemoglobin, INR(PT), MCH, MCHC, MCV, Platelet Count, PT, PTT, RDW, Red Blood Cells, White Blood Cells
Renal failure	Bicarbonate, Calcium (total), Chloride, Creatinine, Glucose, Magnesium, Phosphate, Potassium, Sodium, Troponin T, Urea Nitrogen, Hematocrit, Hemoglobin, INR(PT), MCH, MCHC, MCV, Platelet Count, PT, PTT, RDW, Red Blood Cells, White Blood Cells
Pancreatitis	pO2, Alanine Aminotransferase (ALT), Alkaline Phosphatase, Asparate Aminotransferase (AST), Bicarbonate, Calcium (total), Chloride, Creatine Kinase (CK), Creatinine, Glucose, Lipase, Phosphate, Urea Nitrogen, Hematocrit, Hemoglobin, INR(PT), MCH, MCHC, MCV, Platelet Count, PT, PTT, RDW, Red Blood Cells, White Blood Cells
Respiratory failure	Calculated Total CO2, pCO2, pH, pO2, Bicarbonate, Calcium (total), Chloride, Creatinine, Glucose, Phosphate, Urea Nitrogen, Hematocrit, Hemoglobin, INR(PT), MCH, MCHC, MCV, Neutrophils, Platelet Count, PT, PTT, RDW, Red Blood Cells, White Blood Cells
Ketoacidosis	Calculated Total CO2, pH, pO2, Anion Gap, Bicarbonate, Calcium (total), Chloride, Creatinine, Glucose, Magnesium, Phosphate, Potassium, Sodium, Urea Nitrogen, Hematocrit, Hemoglobin, MCH, MCHC, Platelet Count, RDW, Red Blood Cells, White Blood Cells

Table 4 Medicine item.

Acute complication	Medicine item
Cerebral hemorrhage	Acetaminophen, Bisacodyl, Calcium Gluconate, Docusate Sodium, Famotidine, HydrALAzine, Insulin, Labetalol, LeVETiracetam, Magnesium Sulfate, Metoprolol Tartrate, Potassium Chloride, Propofol, Senna, Sodium Chloride 0.9% Flush
Heart failure	Acetaminophen, Albuterol 0.083% Neb Soln, Aspirin, Docusate Sodium, Furosemide, Heparin, Insulin, Lisinopril, Magnesium Sulfate, Metoprolol Tartrate, Potassium Chloride, Senna, Sodium Chloride 0.9% Flush, Torsemide, Warfarin
Renal failure	Acetaminophen, Aspirin, Dextrose 50%, Docusate Sodium, Furosemide, Heparin, Insulin, Magnesium Sulfate, Metoprolol Tartrate, Ondansetron, OxycoDONE (Immediate Release), Potassium Chloride, Senna, Sodium Chloride 0.9% Flush, Warfarin
Pancreatitis	Acetaminophen, Docusate Sodium, Furosemide, HYDROmorphone (Dilaudid), Heparin, Insulin, Lorazepam, Magnesium Sulfate, Metoprolol Tartrate, Morphine Sulfate, Ondansetron, Pantoprazole, Potassium Chloride, Senna, Sodium Chloride 0.9% Flush,
Respiratory failure	Acetaminophen, Albuterol 0.083% Neb Soln, Calcium Gluconate, Fentanyl Citrate, Furosemide, Heparin, Insulin, Lorazepam, Magnesium Sulfate, Metoprolol Tartrate, Midazolam, Potassium Chloride, Propofol, Sodium Chloride 0.9% Flush, Vancomycin
Ketoacidosis	Acetaminophen, Dextrose 50%, Glucagon, HYDROmorphone (Dilaudid), Heparin, Insulin, Insulin Human Regular, Lorazepam, Magnesium Sulfate, Metoclopramide, Neutra-Phos, Ondansetron, Potassium Chloride, Senna, Sodium Chloride 0.9% Flush

Table 5 Patient biomarkers record.

Time	50809	50818	50820	50821	50882
12/5/2147 2:00	87.5	24	7.44	63	16
12/5/2147 2:52	87.5	24	7.45	121	16
12/5/2147 9:04	121	27	7.42	123	16
12/5/2147 16:31	166	23	7.46	117	16
12/5/2147 17:23	87.5	22	7.46	145	16

Table 6 Patient medication record.

Time	Acetaminophen	HydrALAZine	Insulin	Senna	Sodium chloride
12/12/2147 6:00	0	1	0	0	0
12/12/2147 19:00	0	1	0	1	1
15/12/2147 2:00	1	0	0	0	0
21/12/2147 11:00	0	0	1	0	0
21/12/2147 23:00	0	0	1	0	0

for drug records were filled with zero. In the data preprocessing section, biomarker records and patient continuous demographic information were normalized. Next, discrete demographic information of patients, such as gender, marital status, and ethnicity, were one-hot coded.

The average number of patient visits varies across acute complications. Therefore the size of each acute complication dataset is different. The CLSTM-BPR model needs to construct training and test sets for Model 1, Model 2, and Model 3, seperately. Take the example of Patient 10 078 115 with acute cerebral hemorrhage. Model 1 extracts the 31st to the 2nd data from the bottom for all patients and uses this to predict their last data. The training set is all other patients' data and the test set is Patient 10 078 115's data. Model 2, as shown in Fig. 4, takes every 15 entries for Patient 10 078 115 and predicts the next entry. Patient 10 078 115 has 53 visit records, so 38 sets of data could be taken out. The training set is the first 37 groups, and the test set is the last group. Model 3 splices the output of Model 1 and the output of Model 2 to predict the next visit sign marker values for Patient 10 078 115. The training set for Model 3 is all other patient data and the test set is the data for Patient 10 078 115. The numbers of visits used for Model 1 and Model 2 prediction for different complications are shown in Table 7.

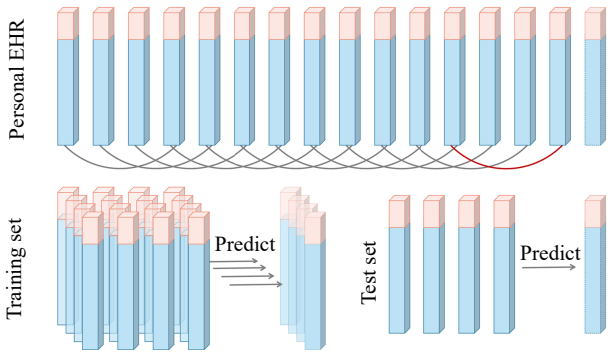

Fig. 4 Schematic diagram of training set and test set division in personal EHR.

Table 7 Number of visits used to predict.

Acute complication	Model 1	Model 2
Acute cerebral hemorrhage	30	15
Acute heart failure	58	20
Acute renal failure	41	10
Acute pancreatitis	31	15
Acute respiratory failure	29	15
Acute ketoacidosis	43	15

5 Result

In this section, we validate the ability of the proposed CLSTM-BPR to predict acute complications in patients with chronic diseases. In terms of prediction, the predictive ability of CLSTM is evaluated from two perspectives: numerical error and abnormality judgment. The superiority of the proposed method is verified by performing comparison experiments and ablation experiments. On the diagnostic side, the reliability of CLSTM-BPR is demonstrated by combining CLSTM with multiple classifiers and performing comparative experiments. The results demonstrated that introducing pairwise algorithms into medical diagnostics is effective.

5.1 Selection of model performance evaluation indices

We used the Mean Square Error (MSE), Root Mean Square Error (RMSE), and MAE as the evaluation indices for prediction. ACC, precision, recall, F1 score (F1), Area Under the Curve (AUC), and Jaccard are used as indicators to assess abnormal biomarker predictive capability and diagnostic capacity.

5.2 Evaluation of the prediction performance

To verify the superiority of this model, the forecasting method of this model is compared with other time-series forecasting models. A representative of machine learning time series forecasting is Vector AutoRegressive Moving Average with exogenous regressors (VARMAX), which is an extension of the

VAR model, incorporating exogenous variables that can affect the dependent variables. It enables the modeling of complex systems with multiple interrelated time series and external factors. VARMAX models are commonly used in economics and finance for forecasting economic indicators. As a representative of deep learning time series forecasting, the LSTM network is also one of the comparison objects. Like CLSTM, LSTM is used separately on public EHR and personal EHR, while VARMAX is only applicable to individual EHR.

At the same time, to demonstrate that it is necessary for the model to consider both disease commonality and individual characteristics, we do ablation experiments. The results of the experiments are shown in Fig. 5 and Table 8, where CLSTM-model 1 denotes the prediction model considering only individual characteristics and CLSTM-model 2 denotes the prediction model considering only disease commonality.

As shown by the mean MSE of 0.412 and RMSE of 0.426, the predictive power of CLSTM is much higher than those of VARMAX and LSTM. Firstly, CLSTM obtains an MSE of less than 1 and an MAE of less than 0.4 in the prediction of all six acute complications. In particular, CLSTM achieves an error of only 0.264 for pancreatitis, which is more than three times smaller than other models. In the ablation experiment, the RMSE of CLSTM is more than 25 times smaller than that of CLSTM-model 1 and more than 2 times smaller than that of CLSTM-model 2. This further demonstrates the necessity of fusing disease commonality and patient characteristics to improve prediction accuracy. And, by contrast, disease commonality plays a greater role in prediction. Further, although the MAEs of LSTM-public and CLSTM-model 2 in Fig. 5 are small enough, their MSEs are 82 times larger than that of CLSTM.

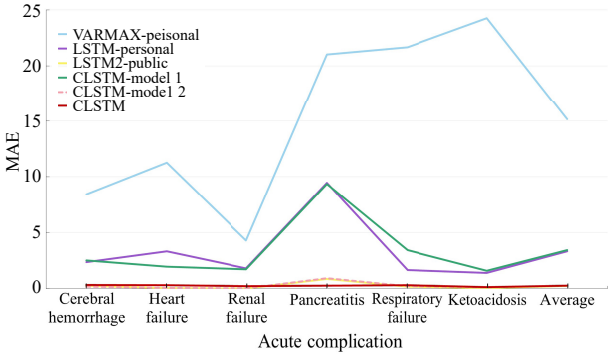

Fig. 5 Comparison of the MAE of biomarkers prediction.

Table 8 Comparison of biomarker prediction results.

Model	Acute complication	Evaluation indice		
		MSE	RMSE	MAE
VARMAX-personal	Cerebral hemorrhage	1487.873	27.217	8.422
	Heart failure	762.572	27.615	11.250
	Renal failure	219.312	11.650	4.302
	Pancreatitis	4799.217	51.774	21.020
	Respiratory failure	18372.434	58.951	21.675
	Ketoacidosis	21472.064	65.719	24.264
	Average	7852.245	40.488	15.155
LSTM-personal	Cerebral hemorrhage	278.743	7.565	2.363
	Heart failure	341.938	10.003	3.335
	Renal failure	203.996	5.718	1.811
	Pancreatitis	5995.430	31.073	9.465
	Respiratory failure	138.936	5.443	1.653
	Ketoacidosis	104.661	4.040	1.394
	Average	1177.284	10.640	3.337
LSTM-public	Cerebral hemorrhage	6.859	1.131	0.252
	Heart failure	0.058	0.144	0.052
	Renal failure	0.007	0.044	0.015
	Pancreatitis	162.588	3.388	0.866
	Respiratory failure	27.193	0.623	0.128
	Ketoacidosis	0.281	0.159	0.056
	Average	32.831	0.915	0.235
CLSTM-model 1	Cerebral hemorrhage	273.520	7.986	2.523
	Heart failure	170.179	6.447	1.953
	Renal failure	124.405	5.268	1.717
	Pancreatitis	6534.407	31.239	9.346
	Respiratory failure	395.252	10.531	3.432
	Ketoacidosis	118.092	4.663	1.587
	Average	1269.309	11.022	3.426
CLSTM-model 2	Cerebral hemorrhage	4.692	0.654	0.181
	Heart failure	0.172	0.184	0.061
	Renal failure	0.017	0.074	0.023
	Pancreatitis	163.230	3.663	0.937
	Respiratory failure	288.250	0.811	0.218
	Ketoacidosis	5.634	0.380	0.104
	Average	33.666	0.961	0.254
CLSTM	Cerebral hemorrhage	0.474	0.510	0.335
	Heart failure	0.269	0.404	0.300
	Renal failure	0.110	0.298	0.215
	Pancreatitis	0.468	0.489	0.264
	Respiratory failure	0.952	0.594	0.317
	Ketoacidosis	0.201	0.258	0.130
	Average	0.412	0.426	0.260

This is because for individual patients, LSTM-public and CLSTM-model 2 exhibit larger errors. Whereas, the prediction error of CLSTM can be controlled to a small value for all patients, which is of importance in medical applications.

After predicting the values, we identify whether the biomarker values are abnormal against the normal range of biomarker values in MIMIC-IV. "1" is used to indicate abnormal and "0" to indicate normal. Comparison with the real abnormal biomarker status yields the results shown in Table 9 and Fig. 6.

It can be found that chronic disease patients without acute complications have better predictive results than those with acute complications. This is in line with the reality that biomarker values are more stable and easier to predict in the absence of acute complications. The average error identification ACC of the six acute complications is 92.6%, indicating a good prediction result. Further analysis reveals that most of the biomarkers that predicted incorrectly are those with small normal ranges. This is because the error of CLSTM is about the same for all biomarkers. However, there are disparities in the normal ranges of different biomarkers. In the case of acute cerebral hemorrhage, for example, with a low MAE of 0.335, the more poorly predicted biomarker terms are pH and INR. Their normal range sizes are 0.1 and 0.2, respectively. Meanwhile, the other 22 items with normal ranges ranging from 0.7 to 290 can be better predicted. How to make accurate prediction of biomarkers with small normal range deserves further study.

5.3 Evaluation of the diagnose performance

To verify the superiority of the disease diagnosis performance of our model, the BPR algorithm of this model is compared with other classifiers for disease diagnosis, including SVM, LR, DT, and NB. The SVM is a binary classification model that maps the feature vector of an instance to some points in space, with the aim of drawing a line that "best" distinguishes between these two types of points. Therefore, if new points become available later, the line can also make a good classification. LR is a very common regression method used to solve binary classification problems, which focuses on finding the optimal parameters to correctly classify the original data. Decision tree is a classification algorithm that creates a tree-like model of decisions and their possible consequences. It works by splitting the data into subsets based on the features and finding the optimal split criteria to build the tree. NB is a classification algorithm that is based on Bayes'

Table 9 Abnormal biomarker identification results.

Acute complication	Target group	Evaluation indicator					
		ACC (%)	Precision	Recall	F1	AUC	Jaccard
Cerebral hemorrhage	Patients with complication	88.1	0.756	0.842	0.787	0.869	0.665
	Patients without complication	92.9	0.716	0.916	0.786	0.924	0.666
	All patients	90.7	0.734	0.882	0.787	0.899	0.665
Heart failure	Patients with complication	88.3	0.767	0.724	0.833	0.892	0.725
	Patients without complication	92.3	0.786	0.938	0.844	0.930	0.756
	All patients	90.4	0.777	0.931	0.839	0.911	0.736
Renal failure	Patients with complication	88.8	0.788	0.919	0.840	0.889	0.741
	Patients without complication	96.1	0.780	0.843	0.790	–	0.700
	All patients	92.9	0.783	0.870	0.808	–	0.715
Pancreatitis	Patients with complication	93.1	0.881	0.949	0.909	0.932	0.841
	Patients without complication	96.5	0.853	0.924	0.878	–	0.809
	All patients	95.1	0.865	0.935	0.891	–	0.823
Respiratory failure	Patients with complication	88.2	0.853	0.890	0.866	0.879	0.772
	Patients without complication	93.1	0.784	0.845	0.795	–	0.683
	All patients	90.9	0.815	0.865	0.827	–	0.723
Ketoacidosis	Patients with complication	91.9	0.886	0.925	0.902	0.915	0.831
	Patients without complication	97.7	0.687	0.574	0.606	–	0.553
	All patients	95.7	0.756	0.695	0.708	–	0.649
Average	–	92.6	0.788	0.863	0.810	0.905	0.719

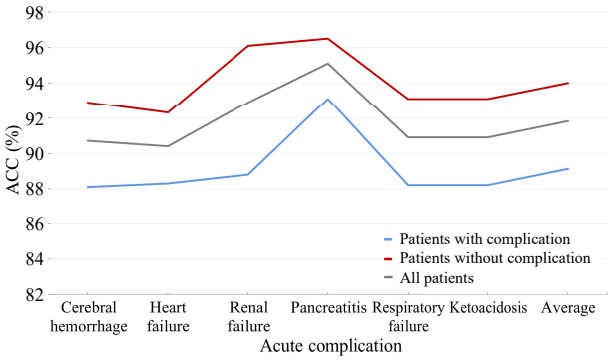

Fig. 6 Comparison of the ACC of abnormal biomarker identification.

theorem. It calculates the probability of each class based on the features of the input data and selects the most probable class as the output. The prediction results of CLSTM output were input into these classifiers to obtain diagnostic results.

The experimental results are shown in Table 10 and Fig. 7. Among five classifiers, the average ACC, F1, AUC, and Jaccard of BPR are higher than those of the other four. It confirms the advantage of BPR as a pairwise algorithm for the application of disease diagnosis. For the four acute complications with the

Table 10 Comparison of diagnosis results.

Model	Diagnosis object	Evaluation indicator					
		ACC (%)	Precision	Recall	F1	AUC	Jaccard
CLSTM-SVM	Cerebral hemorrhage	49.2	0.475	0.983	0.641	0.527	0.472
	Heart failure	47.9	0.479	1.000	0.678	0.500	0.479
	Renal failure	35.9	0.359	1.000	0.528	0.500	0.359
	Pancreatitis	65.3	0.549	1.000	0.709	0.700	0.549
	Respiratory failure	65.6	0.578	0.957	0.721	0.676	0.563
	Ketoacidosis	96.7	0.913	1.000	0.955	0.975	0.913
	Average	60.1	0.559	0.990	0.705	0.646	0.556
CLSTM-LR	Cerebral hemorrhage	85.9	0.936	0.746	0.830	0.851	0.710
	Heart failure	68.8	0.881	0.402	0.552	0.676	0.381
	Renal failure	85.9	0.947	0.643	0.766	0.811	0.621
	Pancreatitis	96.0	1.000	0.904	0.950	0.952	0.904
	Respiratory failure	96.8	0.991	0.940	0.965	0.966	0.932
	Ketoacidosis	91.0	0.816	0.953	0.879	0.920	0.784
	Average	87.4	0.929	0.765	0.824	0.863	0.722
CLSTM-DT	Cerebral hemorrhage	83.6	0.806	0.847	0.826	0.837	0.704
	Heart failure	74.0	0.769	0.652	0.706	0.736	0.545
	Renal failure	85.9	0.793	0.821	0.807	0.851	0.676
	Pancreatitis	83.8	0.857	0.740	0.794	0.825	0.659
	Respiratory failure	96.8	0.966	0.966	0.966	0.968	0.933
	Ketoacidosis	96.7	0.952	0.952	0.952	0.963	0.909
	Average	86.8	0.857	0.830	0.842	0.863	0.738
CLSTM-NB	Cerebral hemorrhage	91.4	0.980	0.831	0.899	0.908	0.817
	Heart failure	75.5	1.000	0.489	0.657	0.745	0.489
	Renal failure	94.6	1.000	0.857	0.923	0.929	0.857
	Pancreatitis	94.2	0.985	0.877	0.928	0.933	0.865
	Respiratory failure	98.0	1.000	0.950	0.978	0.978	0.957
	Ketoacidosis	99.2	1.000	0.976	0.988	0.988	0.976
	Average	92.2	0.994	0.830	0.896	0.914	0.827
CLSTM-BPR	Cerebral hemorrhage	96.9	0.982	0.949	0.966	0.967	0.933
	Heart failure	87.5	0.798	0.989	0.883	0.880	0.791
	Renal failure	95.8	0.931	0.964	0.947	0.959	0.900
	Pancreatitis	97.7	0.973	0.973	0.973	0.976	0.947
	Respiratory failure	92.0	0.881	0.957	0.917	0.922	0.847
	Ketoacidosis	85.2	0.700	1.000	0.824	0.888	0.700
	Average	92.5	0.878	0.972	0.918	0.932	0.853

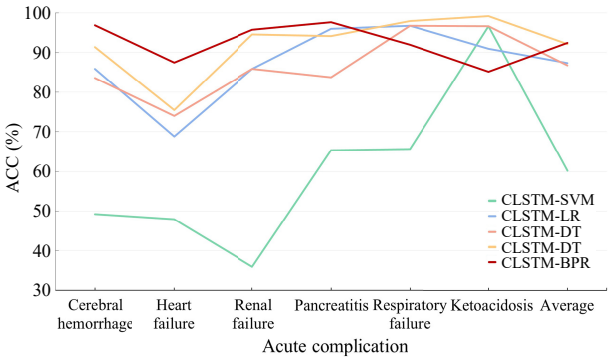

Fig. 7 Comparison of the ACC of disease diagnosis.

highest number of people, the ACC of BPR is higher than those of other classifiers. In particular, BPR is 15.9% more accurate than NB, 18.2% more accurate than DT, 27.2% more accurate than LR, and 82.7% more accurate than SVM in the diagnosis of acute heart failure. Although NB performs well in the diagnosis of the other five acute complications, it is less able to diagnose heart failure. This also proves that BPR has a strong universality in prediction of the six major acute complications. Further analysis reveals that the recall of BPR is higher than the precision. This indicates that BPR is less likely to diagnose patients with chronic disease as acute complications and has a lower misdiagnosis rate. NB, on the contrary, has a higher misdiagnosis rate.

5.4 Comparative analysis

In Table 11, we list some of the complication prediction models from the last five years, along with their methods and effects. Most of the models are designed for individual diseases. For example, Ref. [35] uses the MIMIC-IV database to predict acute kidney injury in patients with diabetic ketoacidosis. It is found that CLSTM-BPR has higher predictive power for acute renal failure than the existing models[33–36] under the condition of using the MIMIC dataset at the same time. In comparison with the prediction models for multiple complications[37–39], CLSTM-BPR has a broader range of disease prediction. More importantly, the average prediction ACC of CLSTM-BPR is 3.68% higher and the highest prediction ACC is 6% higher than those of the existing models.

6 Conclusion

To address the problem of prediction of acute complications of chronic diseases, this study proposes the CLSTM-BPR model. The model divides prediction and diagnosis into two steps, which is more in line with the diagnosis process of real doctors. A complex network structure is designed in the prediction part, so that the model considers both disease commonality and patient characteristics. In the diagnosis part, we try to introduce the pairwise idea into the disease diagnosis by using BPR as the classifier. The reliability of the model is demonstrated in both the prediction and diagnosis parts by predicting the six acute complications in the MIMIC-IV dataset. The MAE of

Table 11 Comparative analysis.

Model	Reference	Year	Predicted disease	Algorithm	Average result (%)	Highest result (%)
Single-target	Shawwa et al.[33]	2021	Acute kidney injury	Machine learning	58.10	58.10
	Liu et al.[34]	2022	Acute kidney injury	RF	87.07	87.07
	Fan et al.[35]	2023	Acute kidney injury	XGBoost	74.90	74.90
	Peng et al.[36]	2023	Acute kidney failure	RF	95.60	95.60
	Proposed	2023	Acute kidney failure	CLSTM-BPR	95.80	95.80
Multi-target	Talaei-Khoei et al.[37]	2019	Heart failure, cardiac arrest, problems with heart valves	CPMC	88.82	91.00
	Zuo et al.[38]	2022	Diabetic retinopathy, diabetic nephropathy, diabetic peripheral neuropathy, diabetic foot disease, diabetic cardiovascular disease	DPMP-DC	85.18	89.58
	Ito et al.[39]	2023	Neurological complications, all complications	DLM	83.15	91.70
	Proposed	2023	Acute cerebral hemorrhage, acute heart failure, acute renal failure, acute pancreatitis, acute respiratory failure, acute ketoacidosis	CLSTM-BPR	92.50	97.70

prediction of CLSTM-BPR is as low as 0.26, lower than existing disease prediction models. Ablation experiments further demonstrate that considering both disease co-morbidities and patient characteristics contributes to more accurate predictions. In comparison with point-pair classifier, BPR not only better diagnoses the four acute complications with the highest number of patients, but also demonstrates generalizability. In conclusion, CLSTM-BPR is of great importance for the prevention of emergent diseases.

There are some shortcomings in this research work, such as the inability to obtain the specific time of onset of sudden illnesses due to differences in the phase interval of patients' medication data. In addition, the predictive effect of the signs and the scores of the sign items derived from the BPR are found to be of medical value in that they may reveal key indicators of disease development. On the one hand, it may help health care professionals to determine the disease, and on the other hand, it may be useful in detecting undetected causative factors. Subsequent studies on these issues will continue.

Acknowledgment

This work was partly supported by the Social Science Fund of China (No. 19BTQ072).

References

[1] J. E. Bennett, V. Kontis, C. D. Mathers, M. Guillot, J. Rehm, K. Chalkidou, A. P. Kengne, R. M. Carrillo-Larco, A. A. Bawah, K. Dain et al., NCD Countdown 2030: Pathways to achieving sustainable development goal target 3.4, *Lancet*, vol. 396, no. 10255, pp. 918–934, 2020.

[2] V.-A. Lioutas, A. S. Beiser, H. J. Aparicio, J. J. Himali, M. H. Selim, J. R. Romero, and S. Seshadri, Assessment of incidence and risk factors of intracerebral hemorrhage among participants in the Framingham heart study between 1948 and 2016, *JAMA Neurol.*, vol. 77, no. 10, p. 1252, 2020.

[3] M. S. Kim, J. H. Lee, H. J. Cho, J. Y. Cho, J. O. Choi, K. K. Hwang, B. S. Yoo, S. M. Kang, and D. J. Choi, KSHF guidelines for the management of acute heart failure: Part III. specific management of acute heart failure according to the etiology and co-morbidity, *Korean Circ. J.*, vol. 49, no. 1, pp. 46–68, 2019.

[4] P. Thapa, K. C. Sudhamshu, A. B. Hamal, D. Sharma, S. Khadka, N. Karki, B. Jaishi, P. S. Tiwari, A. Vaidya, and B. Karki, Prevalence of acute kidney injury in patients with liver cirrhosis, *J. Nepal Med. Assoc.*, vol. 58, no. 228, p. 554, 2020.

[5] WHO, Noncommunicable diseases, https://www.who.int/en/news-room/factsheets/detail/noncommunicable-diseases, 2022.

[6] J. Rashid, S. Batool, J. Kim, M. Wasif Nisar, A. Hussain, S. Juneja, and R. Kushwaha, An augmented artificial intelligence approach for chronic diseases prediction, *Front. Public Health*, vol. 10, p. 860396, 2022.

[7] Y. Zhang, X. Yang, J. Ivy, and M. Chi, ATTAIN: attention-based time-aware LSTM networks for disease progression modeling, in *Proc. Twenty-Eighth Int. Joint Conf. Artificial Intelligence*, Macao, China, pp. 4369–4375, 2019.

[8] K. Li, J. Daniels, C. Liu, P. Herrero, and P. Georgiou, Convolutional recurrent neural networks for glucose prediction, *IEEE J. Biomed. Health Inform.*, vol. 24, no. 2, pp. 603–613, 2020.

[9] K. C. Koo, K. S. Lee, S. Kim, C. Min, G. R. Min, Y. H. Lee, W. K. Han, K. H. Rha, S. J. Hong, S. C. Yang et al., Long short-term memory artificial neural network model for prediction of prostate cancer survival outcomes according to initial treatment strategy: Development of an online decision-making support system, *World J. Urol.*, vol. 38, no. 10, pp. 2469–2476, 2020.

[10] J. J. Lee, J. H. Heo, J. H. Han, B. R. Kim, H. Y. Gwon, and Y. R. Yoon, Prediction of ankle brachial index with photoplethysmography using convolutional long short term memory, *J. Med. Biol. Eng.*, vol. 40, no. 2, pp. 282–291, 2020.

[11] Y. A. Choi, S. J. Park, J. A. Jun, C. S. Pyo, K. H. Cho, H. S. Lee, and J. H. Yu, Deep learning-based stroke disease prediction system using real-time bio signals, *Sensors*, vol. 21, no. 13, p. 4269, 2021.

[12] S. Dutta, J. K. Mandal, T. H. Kim, and S. K. Bandyopadhyay, Breast cancer prediction using stacked GRU-LSTM-BRNN, *Appl. Comput. Syst.*, vol. 25, no. 2, pp. 163–171, 2020.

[13] S. Mohan, C. Thirumalai, and G. Srivastava, Effective heart disease prediction using hybrid machine learning techniques, *IEEE Access*, vol. 7, pp. 81542–81554, 2019.

[14] Y. Ge, Q. Wang, L. Wang, H. Wu, C. Peng, J. Wang, Y. Xu, G. Xiong, Y. Zhang, and Y. Yi, Predicting post-stroke pneumonia using deep neural network approaches, *Int. J. Med. Inform.*, vol. 132, p. 103986, 2019.

[15] E. Choi, A. Schuetz, W. F. Stewart, and J. Sun, Medical concept representation learning from electronic health records and its application on heart failure prediction, arXiv preprint arXiv: 1602.03686, 2016.

[16] Y. Jin, C. Qin, Y. Huang, W. Zhao, and C. Liu, Multi-domain modeling of atrial fibrillation detection with twin attentional convolutional long short-term memory neural networks, *Knowl. Based Syst.*, vol. 193, p. 105460, 2020.

[17] W. Wang, M. Tong, and M. Yu, Blood glucose prediction with VMD and LSTM optimized by improved particle swarm optimization, *IEEE Access*, vol. 8, pp. 217908–217916, 2020.

[18] N. A. Othman, M. A. Abdel-Fattah, and A. T. Ali, A hybrid deep learning framework with decision-level fusion for breast cancer survival prediction, *Big Data Cogn. Comput.*, vol. 7, no. 1, p. 50, 2023.

[19] M. Mahmudimanesh, M. Mirzaee, A. Dehghan, and A. Bahrampour, Forecasts of cardiac and respiratory mortality in Tehran, Iran, using ARIMAX and CNN-

LSTM models, *Environ. Sci. Pollut. Res. Int.*, vol. 29, no. 19, pp. 28469–28479, 2022.
[20] G. Swapna, R. Vinayakumar, and S. K. P, Diabetes detection using deep learning algorithms, *ICT Express*, vol. 4, no. 4, pp. 243–246, 2018.
[21] D. de A. Rodrigues, R. F. Ivo, S. C. Satapathy, S. Wang, J. Hemanth, and P. P. R. Filho, A new approach for classification skin lesion based on transfer learning, deep learning, and IoT system, *Pattern Recognit. Lett.*, vol. 136, pp. 8–15, 2020.
[22] T. H. H. Aldhyani, A. S. Alshebami, and M. Y. Alzahrani, Soft clustering for enhancing the diagnosis of chronic diseases over machine learning algorithms, *J. Healthc. Eng.*, vol. 2020, p. 4984967, 2020.
[23] W. Yue, Z. Wang, H. Chen, A. Payne, and X. Liu, Machine learning with applications in breast cancer diagnosis and prognosis, *Designs*, vol. 2, no. 2, p. 13, 2018.
[24] A. Nithya, A. Appathurai, N. Venkatadri, D. R. Ramji, and C. A. Palagan, Kidney disease detection and segmentation using artificial neural network and multi-kernel k-means clustering for ultrasound images, *Measurement*, vol. 149, p. 106952, 2020.
[25] L. W. Braun, M. A. T. Martins, J. Romanini, P. V. Rados, M. D. Martins, and V. C. Carrard, Continuing education activities improve dentists' self-efficacy to manage oral mucosal lesions and oral cancer, *Eur. J. Dent. Educ.*, vol. 25, no. 1, pp. 28–34, 2021.
[26] G. Battineni, G. G. Sagaro, N. Chinatalapudi, and F. Amenta, Applications of machine learning predictive models in the chronic disease diagnosis, *J. Pers. Med.*, vol. 10, no. 2, p. 21, 2020.
[27] R. R. Janghel and Y. K. Rathore, Deep convolution neural network based system for early diagnosis of Alzheimer's disease, *IRBM*, vol. 42, no. 4, pp. 258–267, 2021.
[28] H. Kanegae, K. Suzuki, K. Fukatani, T. Ito, N. Harada, and K. Kario, Highly precise risk prediction model for new-onset hypertension using artificial intelligence techniques, *J. Clin. Hypertens.*, vol. 22, no. 3, pp. 445–450, 2020.
[29] J. Liu, Z. Yang, T. Li, D. Wu, and R. Wang, SPR: Similarity pairwise ranking for personalized recommendation, *Knowl. Based Syst.*, vol. 239, p. 107828, 2022.
[30] B. Liu and B. Wang, Pairwise learning for personalized ranking with noisy comparisons, *Inf. Sci.*, vol. 623, pp. 242–257, 2023.
[31] L. Li, A. Ayiguli, Q. Luan, B. Yang, Y. Subinuer, H. Gong, A. Zulipikaer, J. Xu, X. Zhong, J. Ren et al., Prediction and diagnosis of respiratory disease by combining convolutional neural network and Bi-directional long short-term memory methods, *Front. Public Health*, vol. 10, p. 881234, 2022.
[32] K. B. Dsouza, A. Maslova, E. Al-Jibury, M. Merkenschlager, V. K. Bhargava, and M. W. Libbrecht, Learning representations of chromatin contacts using a recurrent neural network identifies genomic drivers of conformation, *Nat. Commun.*, vol. 13, no. 1, p. 3704, 2022.
[33] K. Shawwa, E. Ghosh, S. Lanius, E. Schwager, L. Eshelman, and K. B. Kashani, Predicting acute kidney injury in critically ill patients using comorbid conditions utilizing machine learning, *Clin. Kidney J.*, vol. 14, no. 5, pp. 1428–1435, 2021.
[34] W. T. Liu, X. Q. Liu, T. T. Jiang, M. Y. Wang, Y. Huang, Y. L. Huang, F. Y. Jin, Q. Zhao, Q. Y. Wu, B. C. Liu et al., Using a machine learning model to predict the development of acute kidney injury in patients with heart failure, *Front. Cardiovasc. Med.*, vol. 9, p. 911987, 2022.
[35] T. Fan, J. Wang, L. Li, J. Kang, W. Wang, and C. Zhang, Predicting the risk factors of diabetic ketoacidosis-associated acute kidney injury: A machine learning approach using XGBoost, *Front. Public Health*, vol. 11, p. 1087297, 2023.
[36] C. Peng, F. Yang, L. Li, L. Peng, J. Yu, P. Wang, and Z. Jin, A machine learning approach for the prediction of severe acute kidney injury following traumatic brain injury, *Neurocrit. Care*, vol. 38, no. 2, pp. 335–344, 2023.
[37] A. Talaei-Khoei, M. Tavana, and J. M. Wilson, A predictive analytics framework for identifying patients at risk of developing multiple medical complications caused by chronic diseases, *Artif. Intell. Med.*, vol. 101, p. 101750, 2019.
[38] M. Zuo, W. Zhang, Q. Xu, and D. Chen, Deep personal multitask prediction of diabetes complication with attentive interactions predicting diabetes complications by multitask-learning, *J. Healthc. Eng.*, vol. 2022, p. 5129125, 2022.
[39] S. Ito, H. Nakashima, T. Yoshii, S. Egawa, K. Sakai, K. Kusano, S. Tsutui, T. Hirai, Y. Matsukura, K. Wada, et al., Deep learning-based prediction model for postoperative complications of cervical posterior longitudinal ligament ossification, *Eur. Spine J.*, vol. 32, no. 11, pp. 3797–3806, 2023.

Xi Chen received the BE degree from Nanjing Agricultural University, China in 2021. She is currently a master student at School of Economics and Management, Fuzhou University, China. Her research interests focus on recommendation system and artificial intelligence healthcare.

Quan Cheng received the PhD degree in information science from Wuhan University, Wuhan, China in 2009. Currently, he is a professor at School of Economics and Management, Fuzhou University, China. His current research interests include data mining and application of artificial intelligence.